Monthly Notices
of the
ROYAL ASTRONOMICAL SOCIETY

MNRAS **454,** 2606–2620 (2015) doi:10.1093/mnras/stv2221

Kepler observations of A–F pre-main-sequence stars in Upper Scorpius: discovery of six new δ Scuti and one γ Doradus stars

V. Ripepi,[1⋆] L. Balona,[2] G. Catanzaro,[3⋆] M. Marconi,[1⋆] F. Palla[4] and M. Giarrusso[5]

[1]*INAF-Osservatorio Astronomico di Capodimonte, Via Moiariello 16, I-80131 Napoli, Italy*
[2]*South African Astronomical Observatory, PO Box 9, Observatory, Cape Town 7935, South Africa*
[3]*INAF-Osservatorio Astrofisico di Catania, Via S.Sofia 78, I-95123 Catania, Italy*
[4]*INAF-Osservatorio Astrofisico di Arcetri, Largo Enrico Fermi 5, I-50125 Firenze, Italy*
[5]*Università degli studi di Catania, Via S.Sofia 78, I-95123 Catania, Italy*

Accepted 2015 September 22. Received 2015 September 22; in original form 2015 August 4

ABSTRACT

We present light curves and periodograms for 27 stars in the young Upper Scorpius association (age = 11 ± 1 Myr) obtained with the *Kepler* spacecraft. This association is only the second stellar grouping to host several pulsating pre-main-sequence (PMS) stars which have been observed from space. From an analysis of the periodograms, we identify six δ Scuti variables and one γ Doradus star. These are most likely PMS stars or else very close to the zero-age main sequence. Four of the δ Scuti variables were observed in short-cadence mode, which allows us to resolve the entire frequency spectrum. For these four stars, we are able to infer some qualitative information concerning their ages. For the remaining two δ Scuti stars, only long-cadence data are available, which means that some of the frequencies are likely to be aliases. One of the stars appears to be a rotational variable in a hierarchical triple system. This is a particularly important object, as it allows the possibility of an accurate mass determination when radial velocity observations become available. We also report on new high-resolution echelle spectra obtained for some of the stars of our sample.

Key words: stars: fundamental parameters – stars: oscillations – stars: pre-main-sequence – stars: variables: δ Scuti – stars: variables: T Tauri, Herbig Ae/Be.

1 INTRODUCTION

A complete understanding of the star formation process requires the ability to predict how the properties of young stars depend on their initial conditions. Despite significant efforts, a key observational problem remains: the reliable determination of the masses and ages of the youngest pre-main-sequence (PMS) stars once they become optically visible, after the main accretion phase. Stellar masses are needed to investigate the shape of the initial mass function (IMF) and its possible dependence on the properties of the parent cloud. However, obtaining reliable stellar masses is a very difficult task. The only direct method is to use eclipsing binary systems where individual masses of the components can be obtained with great accuracy from the radial velocity and light curve. However, eclipsing systems for PMS stars are rare. Another commonly adopted procedure is to locate the stars in the Hertzpung–Russell (HR) diagram, using estimates of their effective temperatures and luminosities. Masses can be obtained by comparing their position in the HR diagram with theoretical evolutionary tracks, assuming the chemical composition (Hillenbrand & White 2004).

Recently, considerable advances have been made in our understanding of PMS evolution (Palla & Stahler 1999; Siess, Dufour & Forestini 2000; Baraffe et al. 2002; Tognelli, Prada Moroni & Degl'Innocenti 2011). However, differences in the evolutionary tracks remain due to the different treatment of convection, different opacities and differences in the zero point of the calculated ages. This results in considerable differences in mass estimates of single stars from their effective temperatures and luminosities. Without adequate observational constraints, it is impossible to determine the correct assumptions in the evolutionary model calculations. For this reason, it is very important to obtain independent determinations of PMS masses and ages.

In this context, intermediate-mass PMS stars (with mass in the range 1–8 $M_{\odot}$, also called Herbig Ae/Be stars) are particularly useful. After the seminal work by Marconi & Palla (1998), who established the locus of the theoretical instability strip in the HR diagram, it has become clear that these stars pulsate as δ Sct variables (see e.g. Ripepi et al. 2002, 2003; Marconi & Palla 2004; Ripepi et al. 2006a,b; Zwintz 2008 and references therein). More recently, high-precision photometry from space missions such as

⋆E-mail: ripepi@oacn.inaf.it (VR); gca@oact.inaf.it (GC); marconi@oacn.inaf.it (MM)

MOST and *CoRoT* showed that intermediate-mass PMS stars can also pulsate as hybrid δ Sct/γ Dor stars (Ripepi et al. 2011) or pure γ Dor stars (Zwintz et al. 2013). This is interesting because the occurrence of low frequencies in δ Sct stars (i.e. hybrid pulsation) was originally thought to be exceptional. However, *Kepler* observations have shown that all δ Sct stars have low frequencies (Balona 2014). The reason why the hybrid concept arose is due to the fact that the low frequencies attain sufficient amplitudes to be visible from the ground only in a narrow temperature range. The mechanism which drives low frequencies in hot δ Sct stars is currently unknown.

The additional information provided by pulsation can be used to construct detailed models of the varying internal structure of these stars as they contract towards the main sequence, in order to compare the predicted frequencies to the observed ones (Ruoppo et al. 2007; Di Criscienzo et al. 2008; Casey et al. 2013). The physics of PMS stellar evolutionary models can therefore be tested. Several efforts have recently been made to analyse the properties of known PMS pulsators (see e.g. Zwintz et al. 2014). However, the analysis is hampered by several factors such as the uneven quality of the observational data (ground and space time-series data have very different properties), the lack of precise spectroscopically derived stellar parameters, the possibly different intrinsic properties of cluster and field PMS pulsators, and difficulties in the treatment of rapidly rotating stars.

In this context, PMS pulsators belonging to clusters or associations are of particular interest, since the member stars share the same chemical composition, age and interstellar absorption, greatly simplifying the comparison between theory and observations. This is the case, for example, of NGC 2264, a well-studied cluster where nine PMS pulsators have been observed from space (Zwintz et al. 2014). The Upper Scorpius association (USco) is perhaps of even greater interest due to the large number of known A–F members (de Zeeuw et al. 1999; Pecaut, Mamajek & Bubar 2012) and the availability of accurate individual distances based on *Hipparcos* parallaxes. Moreover, stellar parameters have been estimated for most of the member stars.

USco is part of the larger Scorpius–Centaurus (Sco–Cen) association, a young (∼5–10 Myr) and relatively close (∼120–150 pc) region of recent star formation (de Bruijne 1999; de Zeeuw et al. 1999) that includes the Upper Centaurus-Lupus (UCL) and Lower Centaurus-Crux (LCC). USco is the youngest of them and contains many intermediate-mass members, making it an ideal target to investigate the whole extension of the PMS instability strip. Indeed, its member stars are sufficiently bright ($\sim 7 < V < 10$ mag) to acquire extremely precise photometry both from the ground and from space.

Due to the loss of a second spacecraft reaction wheel, the *Kepler* satellite ended data collection in the original Cygnus field after four years of continuous monitoring. By pointing near the ecliptic plane, the *Kepler* spacecraft is able to minimize pointing drift, acquiring data with much reduced photometric precision. This mode of operation is called the K2 project.[1] The USco region falls partially within the field of view of the *Kepler* satellite during the *K2-C02* campaign, becoming a primary target for our purposes. In this work, we present the results of a search for pulsating PMS stars among the USco member stars observed by *Kepler*.

The structure of the paper is the following: in Section 2, we describe the *Kepler* data and the techniques of data reduction and analysis; in Section 3, we present the classification of the variables; Section 4 reports a the results of the spectroscopic follow-up for a sample of interesting templates; Section 5 includes a discussion about the evolutionary status of the target stars; Section 6 reports a discussion of the properties of the pulsating stars. Finally, a brief summary closes the paper.

[1] See http://keplerscience.arc.nasa.gov/K2/ for details.

2 *KEPLER* OBSERVATIONS

Kepler observations usually consist of 30-min exposures (long cadence or LC mode), but a few stars can be observed with 1-min exposures (short cadence or SC mode). Observations of 16 PMS stars in USco, 7 of which were also observed in SC mode, were obtained by *Kepler*. The *K2-C02* campaign started on 2014 Aug 23 and ended on 2014 Nov 10, for a total duration of about 78.7 d. The selected stars come from the lists of de Bruijne (1999) and Pecaut et al. (2012). The spectral types of the selected stars range from A2 to F7 (to embrace the entire δ Sct and γ Dor instability strips, taking also into account possible errors on the spectral type values by 1–2 subclasses or more). We also searched the *Kepler K2* data archive at MAST (Mikulski Archive for Space Telescopes) for additional A–F members of USco and found an additional nine objects (two in SC mode), mainly A0 stars, giving a total of 27 USco members. The targets and their main properties are listed in Table 1.

2.1 Data reduction and frequency analysis

Data reduction was carried out by means of the PYKE software (Still & Barclay 2012) and also by our own custom software. Simple aperture photometry (SAP) was extracted from raw pixel files and then corrected for the instrumental signatures present in the data. Spacecraft drift is the main component leading to increased photometric scatter compared to the original *Kepler* field. Using SAP, the brightness of a target changes slowly as the star moves from its original location on the CCD until the thrusters are applied to bring the star back to its original location. The periodogram therefore shows strong peaks at about 4.08 d^{-1} and its harmonics, which corresponds to the frequency at which the thrusters are applied. It is possible to obtain a greatly improved light curve simply by locating these peaks in the periodogram and fitting and removing a truncated Fourier series. Extraction of the light curve from the FITS files using SAP, fitting and removing the truncated Fourier series was done using custom software.

A more sophisticated approach to correct the light curve was proposed by Vanderburg & Johnson (2014). In this technique, the non-uniform pixel response function of the *Kepler* detectors is determined by correlating flux measurements with the spacecraft's pointing and removing the dependence. This leads to an improvement over raw SAP photometry by factors of 2–5, with noise properties qualitatively similar to *Kepler* targets at the same magnitudes. There is evidence that the improvement in photometric precision depends on each target's position in the *Kepler* field of view, with worst precision near the edges of the field. Overall, this technique restores the median-attainable photometric precision within a factor of 2 of the original Kepler photometric precision for targets ranging from 10–15 mag in the *Kepler* bandpass. This technique is implemented in the KEPSFF task within the PYKE software suite. This is the method used in our analysis. Correction of the periodogram of the raw SAP photometry as mentioned above is very useful as a check on possible artefacts which may arise in the KEPSFF task.

The light curves for the 27 targets with LC data are shown in Fig. 1, whereas Fig. 2 displays an enlargement of the light curves for the seven stars with SC data. Periodograms and frequency extraction

Table 1. Stellar parameters for A-type Upper Sco members. The meaning of the different columns is the following: (1) EPIC number; (2) HIP identifiers; (3) mode of observation: LC and SC stands for long and short cadence, respectively; (4) variable classification; (5) *Kepler* magnitude; (6) spectral type; (7) interstellar absorption; (8) parallax; (9) logarithm of the effective temperature; (10) logarithm of the luminosity in solar units. All the data reported in columns (6–10) are from Pecaut et al. (2012); (11) disc classification according to Luhman & Mamajek (2012): d/e = debris/evolved transitional disc; f = full disc.

EPIC	HIP	Mode	Var. type	KepMag	ST	A_V	π	$\log T_{\rm eff}$	$\log L/L_\odot$	Disc
				mag		mag	mas			
(1)	(2)	(3)	(4)	(5)	(6)	(7)	(8)	(9)	(10)	(11)
202842502	79733	LC	–	9.054	A1mA9–F2	1.25 ± 0.04	4.51 ± 0.43	3.964 ± 0.019	1.48 ± 0.092	–
202876718	79878	LC	–	7.183	A0V	0.00 ± 0.02	7.35 ± 0.55	3.980 ± 0.031	1.407 ± 0.07	d/e
203120347	80586	LC	–	8.211	F5IV–V	0.00 ± 0.10	7.02 ± 0.65	3.814 ± 0.011	0.93 ± 0.09	–
203399155	80311	LC	–	8.878	A1V	0.93 ± 0.05	5.51 ± 0.49	3.964 ± 0.019	1.266 ± 0.08	–
203660895	79097	LC	–	9.155	F4V	0.48 ± 0.12	6.99 ± 0.57	3.822 ± 0.009	0.90 ± 0.09	–
203712541	78494	LC	–	7.722	A2mA7–F2	0.75 ± 0.06	7.26 ± 0.57	3.943 ± 0.016	1.395 ± 0.077	–
203774126	80799	LC	–	7.900	A3V	0.25 ± 0.04	7.97 ± 0.62	3.932 ± 0.012	1.078 ± 0.068	d/e
203931628	80196	LC	DSCT	9.030	A1Vn	2.36 ± 0.18	5.94 ± 0.56	3.964 ± 0.019	1.602 ± 0.102	d/e
204054556	79054	LC	GDOR	9.215	F3V	0.35 ± 0.05	6.24 ± 0.53	3.827 ± 0.005	0.78 ± 0.08	d/e
204076987	79643	LC	–	9.393	F3V	0.56 ± 0.05	6.63 ± 0.62	3.827 ± 0.005	0.67 ± 0.08	d/e
204175508	77960	LC	DSCT	8.410	A4IV/V	0.75 ± 0.02	8.56 ± 0.71	3.918 ± 0.012	0.973 ± 0.093	–
204222666	78099	LC	–	7.790	A0V	0.59 ± 0.03	7.42 ± 0.59	3.980 ± 0.031	1.367 ± 0.073	d/e
204239132	80238	LC	–	7.848	A2.5V	0.74 ± 0.09	8.00 ± 0.68	3.937 ± 0.014	1.389 ± 0.081	d/e
204242194	79250	LC	–	7.829	A3III/IV	0.33 ± 0.05	9.60 ± 0.75	3.932 ± 0.012	0.963 ± 0.072	d/e
204372172	80088	LC/SC	DSCT	9.000	A9V	0.61 ± 0.03	6.11 ± 0.66	3.872 ± 0.010	0.960 ± 0.095	d/e
204399980	79476	LC/SC	DSCT/LPV	8.822	A8IVe	1.02 ± 0.40	7.56 ± 0.61	3.875 ± 0.010	1.006 ± 0.175	f
204492384	79644	LC	ROT	10.024	F6V	0.53 ± 0.11	6.30 ± 0.64	3.802 ± 0.007	0.44 ± 0.10	–
204494885	80130	LC/SC	DSCT	8.727	A9V	0.66 ± 0.02	6.41 ± 0.57	3.872 ± 0.010	1.089 ± 0.077	–
204506777	78977	LC/SC	EA/ROT	8.752	F8V	0.38 ± 0.08	7.53 ± 0.64	3.788 ± 0.007	0.83 ± 0.08	–
204638251	80059	LC/SC	DSCT	8.745	A7III/IV	0.56 ± 0.07	7.74 ± 0.64	3.892 ± 0.014	0.907 ± 0.075	–
204662993	79977	LC/SC	–	9.099	F3V	0.36 ± 0.05	7.79 ± 0.66	3.827 ± 0.005	0.63 ± 0.08	d/e
204810792	79083	LC	–	8.226	F3V	0.76 ± 0.13	7.16 ± 0.63	3.827 ± 0.005	1.13 ± 0.09	–
204926239	79606	LC/SC	–	9.039	F8V	0.81 ± 0.14	9.19 ± 0.79	3.788 ± 0.007	0.65 ± 0.09	–
204966512	80019	LC	–	8.396	A0V	1.03 ± 0.07	7.81 ± 0.68	3.980 ± 0.031	1.374 ± 0.084	d/e
205002311	82218	LC	ROT?	9.008	F3V	0.30 ± 0.02	8.39 ± 0.72	3.827 ± 0.005	0.55 ± 0.08	d/e
205089268	79156	LC	–	8.804	A0V	0.60 ± 0.07	6.43 ± 0.54	3.980 ± 0.031	1.366 ± 0.081	d/e
205181377	79124	LC	–	8.630	A0V	0.78 ± 0.05	6.51 ± 0.53	3.980 ± 0.031	1.55 ± 0.078	–

were performed using the PERIOD04 software (Lenz & Breger 2005). The periodograms for these stars are shown in Figs 3 and 4.

Problems in the low-frequency regime may be expected given the image drift. It is therefore important to identify common frequencies in the periodograms which could be of instrumental origin or artefacts of the reduction process. Most of the periodograms obtained from applying the Vanderburg & Johnson (2014) technique have a peak at frequency $\nu = 0.51$ d^{-1} which can be identified as an instrumental frequency. In many stars the peak at half this frequency, $\sim$0.26 d^{-1}, is also present. Stars having this feature include EPIC 202842502, 203660895, 203931628, 204076987, 204494885, 204638251, 204810792 and 205089268. Other artificial peaks are present and these must be recognized in order not to be misled in classifying the star as a variable. In Figs 3 and 4, we have shown with dashed lines the frequencies that are likely of instrumental origin. These are the harmonics of $\nu = 0.51$ d^{-1} and of 4.08 d^{-1}.

3 CLASSIFICATION OF VARIABLES

As an essential first step, it is necessary to examine the periodograms and light curves of all stars in order to identify pulsating variables and other interesting objects. The only pulsating stars in the observed spectral range that can be safely identified are δ Sct (characterized by the presence of one or more high frequencies, i.e. frequencies in excess of about 5 d^{-1}). γ Doradus stars, which have multiple frequencies lower than about 5 d^{-1}, are difficult to identify with certainty. This arises because of the possibility of spurious instrumental frequencies in this range as well as irregular variability caused by circumstellar material which might be present in these young stars. Furthermore, one cannot ignore the possibility that many stars may have spots which have different frequencies due to differential rotation or finite lifetimes. Bearing these difficulties in mind, our attempted classifications are presented in Table 1.

Five stars are definitely δ Sct (DSCT) variables: EPIC 203931628, 204175508, 204372172, 204494885 and 204638251. At a first look, EPIC 204399980 seems to be an irregular long-period variable. However, a closer inspection of the SC light curve and its periodogram (Figs 2 and 4) reveals a very likely δ Sct pulsation with frequencies in the range 30–40 d^{-1} superimposed over irregular variations on a longer time-scale. This kind of photometric behaviour is typical of an Herbig Ae star and is caused by the partial obscuration of the star's photosphere by circumstellar material (see Section 5).

We identify EPIC 204054556 as a γ Dor (GDOR) variable. EPIC 204492384 could be GDOR, but it looks more like a rotational variable (broad multiple peak at $\sim$1.14 d^{-1} and harmonic at $\sim$2.28 d^{-1}). The multiple close frequencies at $\sim$1.14 d^{-1} can be attributed to differential rotation. Similarly, EPIC 205002311 might be a rotational variable because the harmonic is present, but this classification is uncertain due to the low amplitude and the significant noise in this part of the spectrum.

EPIC 204506777 (HD 144548) is a very interesting star. It is an eclipsing binary of Algol type (Kiraga 2012) with period $P = 1.62780$ d and $v \sin i = 80 \pm 5$ km s^{-1}. There are two small amplitude eclipses. From the periodogram, we find a main period

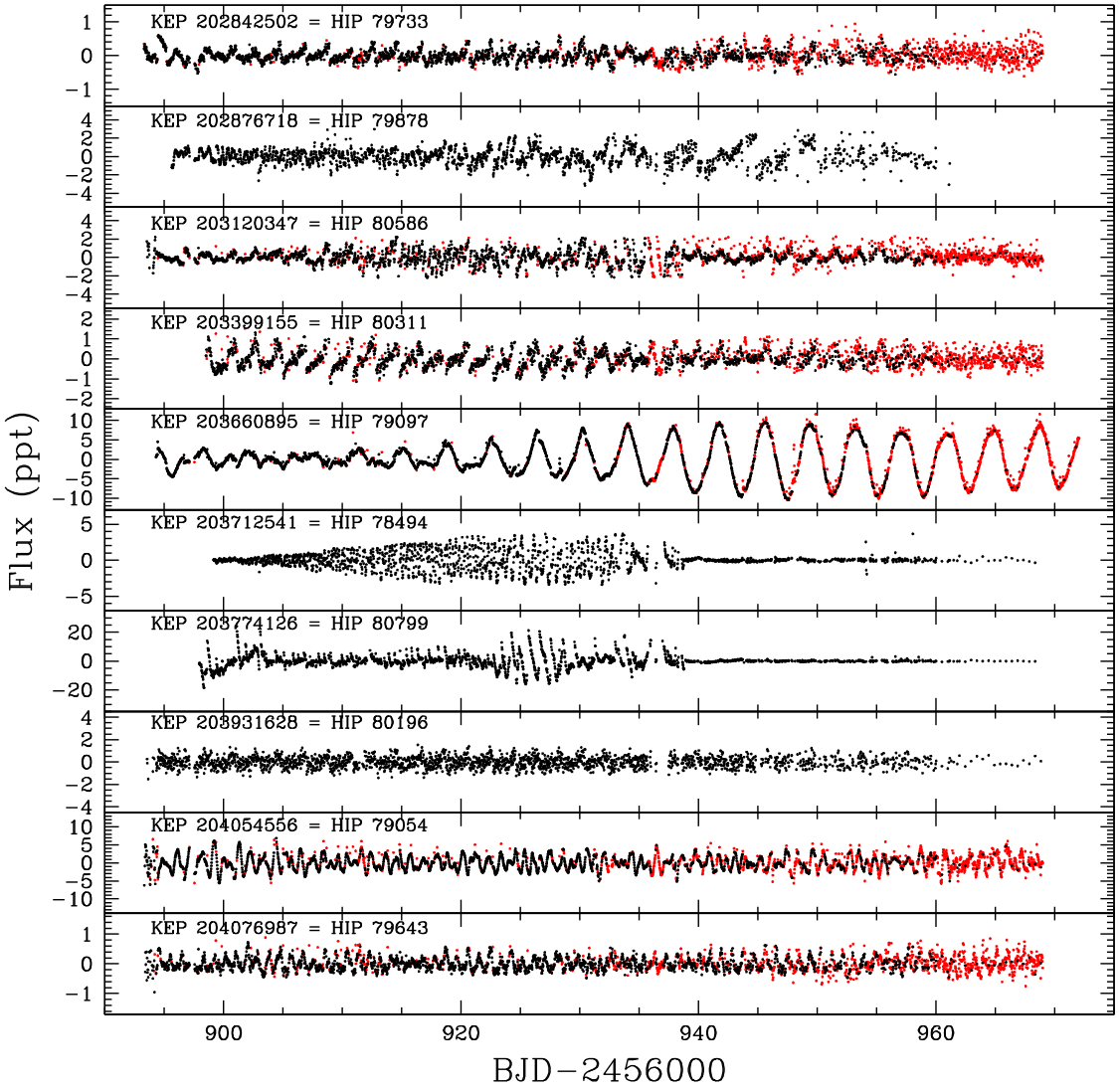

Figure 1. LC light curves for the 27 objects investigated in this paper. Black and red points show data with quality flag equal or greater than zero (flag=0 means optimum quality, see http://archive.stsci.edu/kepler/manuals/archive_manual.pdf for details), respectively. For some objects, the non-zero flag data was omitted because it was too scant.

$P = 1.524(1)$ d. The light curve at this period is roughly sinusoidal and could be interpreted as the rotation period. There also seems to be a short regular eclipses at $P = 1.628(1)$ d (the same period reported by Kiraga 2012, see also Fig. 2). On top of this are deeper eclipses at JD 2064.32 and JD 2124.01 and a secondary *double* eclipse at JD 2089.94 and JD 2090.30. It is not easy to interpret this variability, but possibly what we are seeing is a third body which eclipses a close binary with period 1.628(1) d. The double eclipse is of equal depth, indicating that the close binary has equal components. This is a very interesting system which deserves further study.

4 SPECTROSCOPIC FOLLOW-UP

In the previous section, we identified several interesting stars worth of further analysis, especially the seven pulsating stars and the possible triple system (EPIC 20450677). To fully exploit the potentialities of the *K2* photometry, especially for the pulsating stars, it is important to derive high-resolution spectroscopic estimates of the stellar parameters and of the rotational velocities $v \sin i$. To this aim, we searched the literature and the available web archives for high-resolution spectra of our targets. We found data for two stars.

(i) EPIC 204399980 (HIP 79476 = HD 145718) has been studied spectroscopically in some detail by Carmona et al. (2010). The spectrum displays an inverse P Cygni Hα profile, presumably a result of accretion, confirming the Herbig Ae nature of this star. They obtained a projected rotational velocity, $v \sin i = 100 \pm 10$ km s^{-1} and a centre-of-mass velocity $v_r = 0 \pm 3$ km s^{-1}.

(ii) A spectrum of EPIC 204506777 (HIP 78977 = HD 146897), obtained on 2006 June 20 with the FEROS echelle spectrograph on the 2.2-m Max Planck Gesellschaft telescope (resolution of 48 000, exposure time 90 s) was found in the ESO archive.

Nothing was found for the remaining six pulsating stars. Hence, we decided to observe all of them using the new Catania Astrophysical Observatory Spectropolarimeter (CAOS) facility.

The next section describes these new spectroscopic observations and data analysis for the seven observed stars (see Table 2 for a list). We note that both EPIC 204399980 and EPIC 204506777 were re-observed with CAOS in order to search for duplicity in

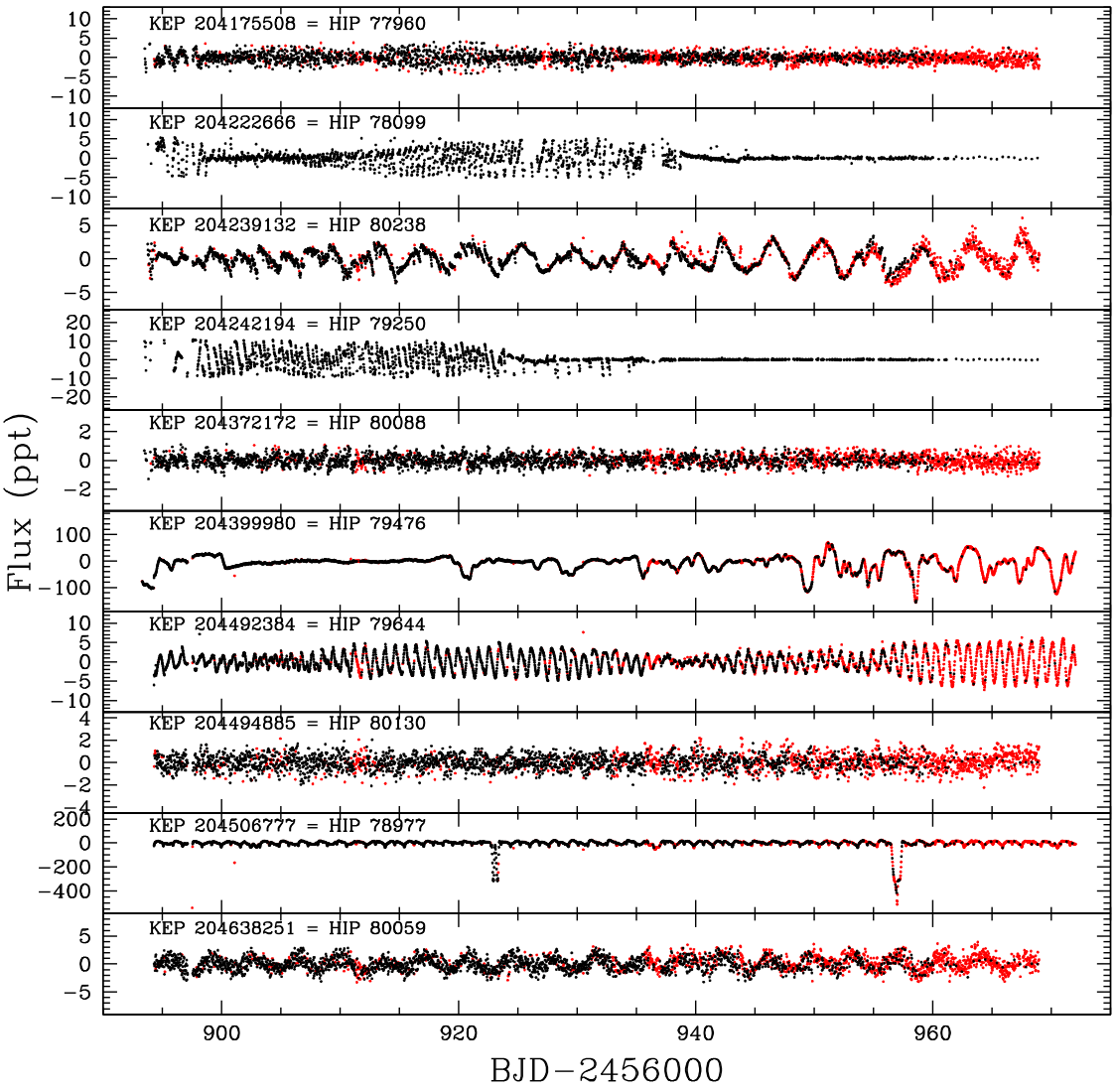

Figure 1 – *continued*

the former star and to compare the spectroscopic results for the latter. We also observed the two stars with SC data which do not pulsate, i.e. EPIC 204662993 and EPIC 204926239. Unfortunately, the weather conditions did not allow observations of the pulsating stars EPIC 203931628, 204054556 and 204175508.

4.1 CAOS spectra

CAOS is a fibre fed, high-resolution spectrograph recently installed at the Cassegrain focus of the 91-cm telescope of the 'M. G. Fracastoro' observing station of the Catania Astrophysical Observatory (Mt Etna, Italy). The spectra were obtained in 2015 June and July. Because the targets were very low above the horizon, they could only be observed for about 1 h. We used an exposure time of 3600 s for all observations. The typical signal-to-noise ratio of the spectra is in the range 40–80 and the resolution $R = 45\,000$ as measured from the ThAr and telluric lines. For details on the spectrograph and the data reduction procedure, see Catanzaro et al. (2015).

The spectrum synthesis approach followed in this paper to derive fundamental stellar parameters is based on the unix port of the ATLAS9-SYNTHE suite of codes (Kurucz 1993a,b; Kurucz & Avrett 1981; Sbordone et al. 2004). This approach has been successfully used in a number of papers in the recent literature (see e.g. Catanzaro et al. 2011, 2015; Catanzaro & Ripepi 2014; Doyle et al. 2014; Hubrig et al. 2014; Niemczura et al. 2015; Paunzen et al. 2014, just to quote some recent work). The website by Fiorella Castelli[2] contains a description of all the improvements of the Kurucz codes and related updates in the input physics performed in the latest years. A comparison between SYNTHE (Kurucz & Avrett 1981) and SYNTH (Valenti & Piskunov 1996) was already performed by Catanzaro, Ripepi & Bruntt (2013), who demonstrated that the results provided by the two codes are perfectly consistent. We also note that the new version of ATLAS, i.e. ATLAS12 (Kurucz 1997), differs from the previous ATLAS9 only in the method adopted to compute the opacity. A comparison between ATLAS9 and ATLAS12 synthesis was performed by e.g. Catanzaro & Balona (2012), who found that the two codes give consistent results if the metallicity of the target star is not far from the adopted solar one.

In this paper, since the targets likely have circumstellar material that could partially fill the Hα line, we have derived the effective temperatures minimizing the difference between observed and

[2] http://www.oact.inaf.it/castelli/

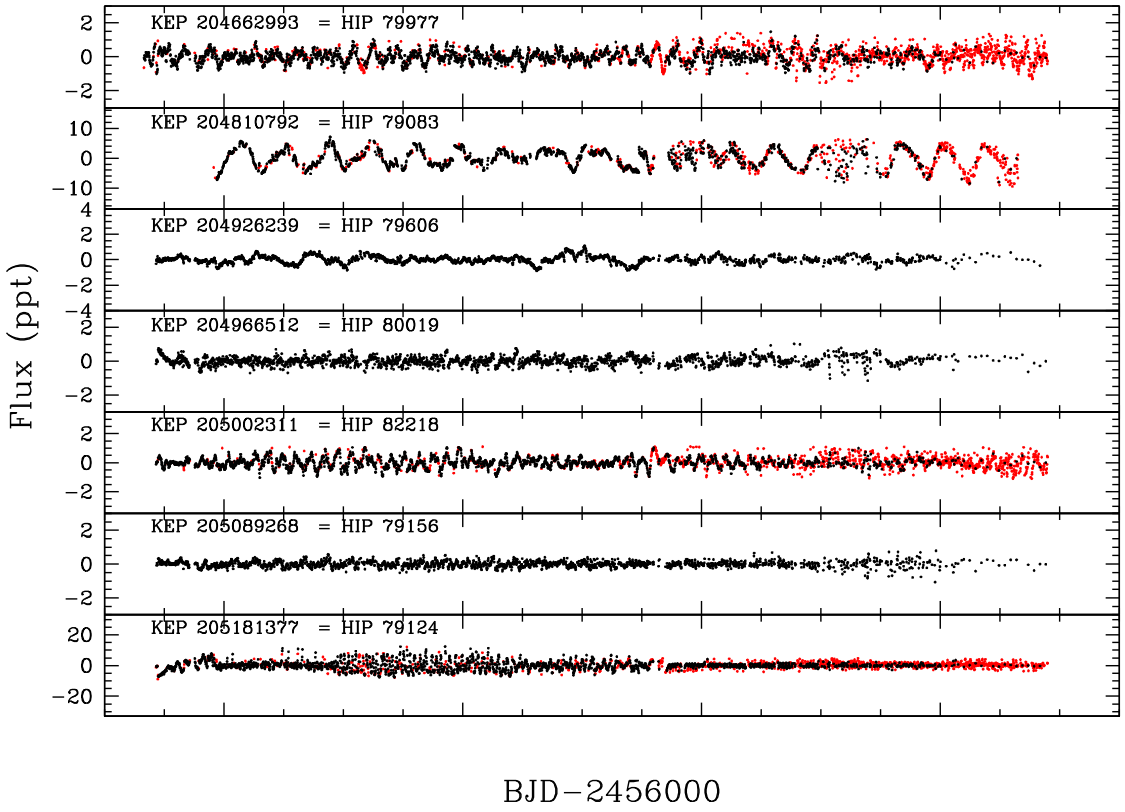

Figure 1 – *continued*

synthetic Hβ profiles, using as goodness-of-fit parameter the χ^2 defined as

$$\chi^2 = \frac{1}{N}\sum\left(\frac{I_{\rm obs} - I_{\rm th}}{\delta I_{\rm obs}}\right) \quad (1)$$

where N is the total number of points, $I_{\rm obs}$ and $I_{\rm th}$ are the intensities of the observed and computed profiles, respectively, and $\delta I_{\rm obs}$ is the photon noise. Synthetic spectra were generated in three steps: (i) we computed Local Thermodynamic Equilibrium (LTE) atmospheric models using the ATLAS9 code; (ii) the stellar spectra were synthesized using SYNTHE; (iii) the spectra were convolved for the instrumental and rotational broadening.[3] We used as initial guesses for temperatures the values derived by Pecaut et al. (2012), that we report for the sake of clarity in Table 2. In Fig. 5, we plot the synthetic profiles (even for Hα) superposed on the observed spectra. Moreover, we computed the $\log g$ and the $v\sin i$ by spectral synthesis of the region around Mg I triplet at $\lambda\lambda$5167–5183 Å (see Fig. 6). The resulting values are listed in Table 2.

In a completely similar way, we analysed the FEROS spectrum for EPIC 204506777 (see Fig. 7), which was obtained in better conditions with respect to the CAOS one (USco is high in sky in the Southern hemisphere). As a result, we found a value of the radial velocity of $V_{\rm rad} = -13.75 \pm 0.49$ km s^{-1} (JD = 245 3906.6783). Comparison with the value reported in Table 2 reveals a clear variation due to the motion of the binary or triple system. Further data will be obtained in the future to build up a complete radial velocity curve.

[3] Only for HIP 79476 this method has not been applied because of the strong emission in the Hα profile and the possible filling of the Hβ. In this case, we use the ionization equilibrium of iron to estimate the effective temperature

An inspection of Table 2 reveals that there is an overall good agreement within the errors between literature (Pecaut et al. 2012, and references therein) and CAOS effective temperatures. The only relevant exceptions are EPIC 204399980 (HIP 79476) and 204494885 (HIP 80130). For the first star, we find an effective temperature about 500 K larger than that reported by Pecaut et al. (2012), who in turn refer to Vieira et al. (2003). However, on the basis of high-resolution spectroscopy, Carmona et al. (2010) discussed the spectral type of this star, concluding that it cannot be later than A5Ve and estimated a $T_{\rm eff}^{\rm spec} = 8200$ K, almost identical to our value. On this basis, we believe that our estimate of $T_{\rm eff}^{\rm spec} = 8100 \pm 300$ K is sound. In passing, we note that our CAOS spectrum allows us to evaluate the possible multiplicity of EPIC 204399980, by comparing our determination of $V_{\rm rad} = -7.4 \pm 6.4$ km s^{-1} with Carmona et al. (2010)'s $V_{\rm rad} = 0 \pm 3$ km s^{-1}. The two values agree within $\sim 1\sigma$, hence we conclude that at least with present data, there is no evidence of multiplicity for this star.

As for EPIC 204494885, the previous effective temperature evaluation dates back to Houk & Smith-Moore (1988) who classified the stars visually on objective-prism plates. Therefore, their effective temperature estimate cannot be accurate. Also in this case, we decided to take our value.

5 EVOLUTIONARY STATUS OF THE INVESTIGATED STARS

In the context of this paper, it is important to establish the evolutionary status of the target stars, particularly those pulsating as δ Sct or γ Dor. Fig. 8 shows the HR diagram for the A- and F-type stars members of the USco association according to analysis of Pecaut et al. (2012). For the stellar parameters, we have adopted the values

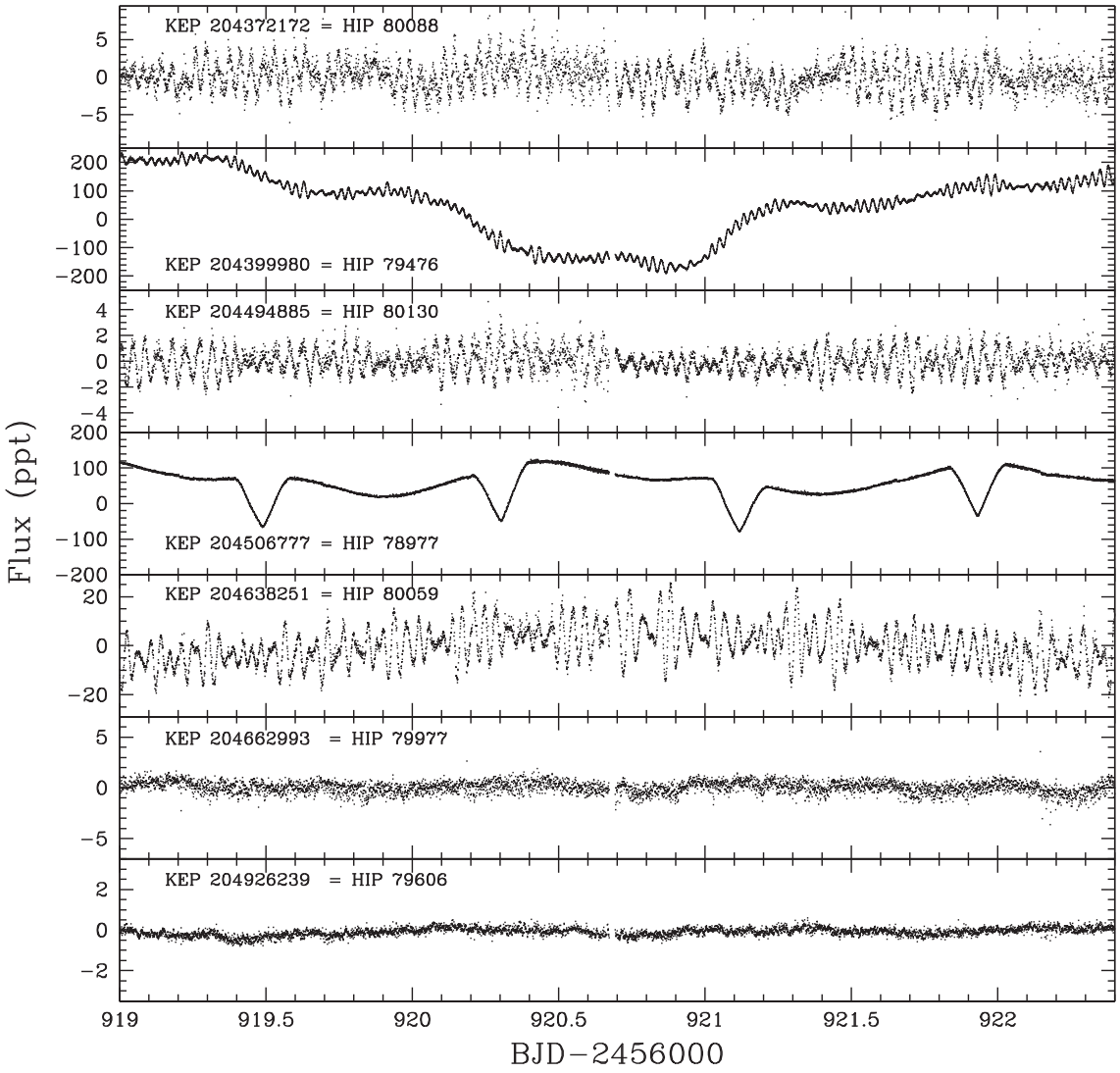

Figure 2. The figure shows selected portion of SC light curves for the seven targets observed in this cadence.

listed in columns (9) and (10) of Table 1, except for the four δ Sct stars for whom we used our spectroscopically determined values. As we discussed in Section 4, there is some disagreement between our own results and those of Pecaut et al. (2012). However, we note that the use of Pecaut et al. (2012) data would not affect significantly our conclusions.

The HR diagram in Fig. 8, includes some selected evolutionary tracks and isochrones from the models by Tognelli et al. (2011). Note that Pecaut et al. (2012) used for their analysis a combination of empirical isochrones and the models of Dotter et al. (2008) and found an age for USco of 11 $\pm$ 1 Myr. As seen in Fig. 8, we confirm this estimate since the position of almost all the A-type stars is compatible within the errors with the 10 Myr isochrone of the models of Tognelli et al. (2011).

So far, we have assumed that all the stars investigated in this paper are in the PMS phase. One can argue that their membership to the USco association should guarantee their youth, considering that not only Pecaut et al. (2012), but also previous studies report an age of 5–10 Myr (see e.g. de Zeeuw et al. 1999; Luhman & Mamajek 2012, and references therein) for this association. However, as a check, we now proceed to provide further evidence on this assumption.

In general, the distinctive properties of young A- and F-type stars (also known as Herbig Ae stars) are the presence of Hα emission (or filling of the line) in their spectrum, a luminosity class III–V, and the presence of excess infrared emission due to circumstellar dust (see e.g. van den Ancker, de Winter & Tjin A Djie 1998, and references therein). Now, all the stars of our sample satisfy the criterion on the luminosity class. As for the presence of Hα emission, only the spectrum of EPIC 204399980 shows it unambiguously (cf. Section 4 and below), whereas for the remaining stars a partial filling of the Hα line cannot be excluded.

The disc population of USco has been thoroughly investigated by Luhman & Mamajek (2012). Their results for the stars in common with our sample are shown in column (11) of Table 1. About half of our stars show the presence of a disc, even if in most cases it is an evolved (debris, transitional) structure, possibly devoid of gas. The only exception is EPIC 204399980 with its clear signature of accretion in the Hα profile. Not surprisingly, its light curve displays long term, irregular photometric variations due to the variable obscuration of the photosphere produced by circumstellar dust, as commonly found among Herbig Ae stars (see e.g. Herbst et al. 1994, and references therein). An obvious interpretation would be that the

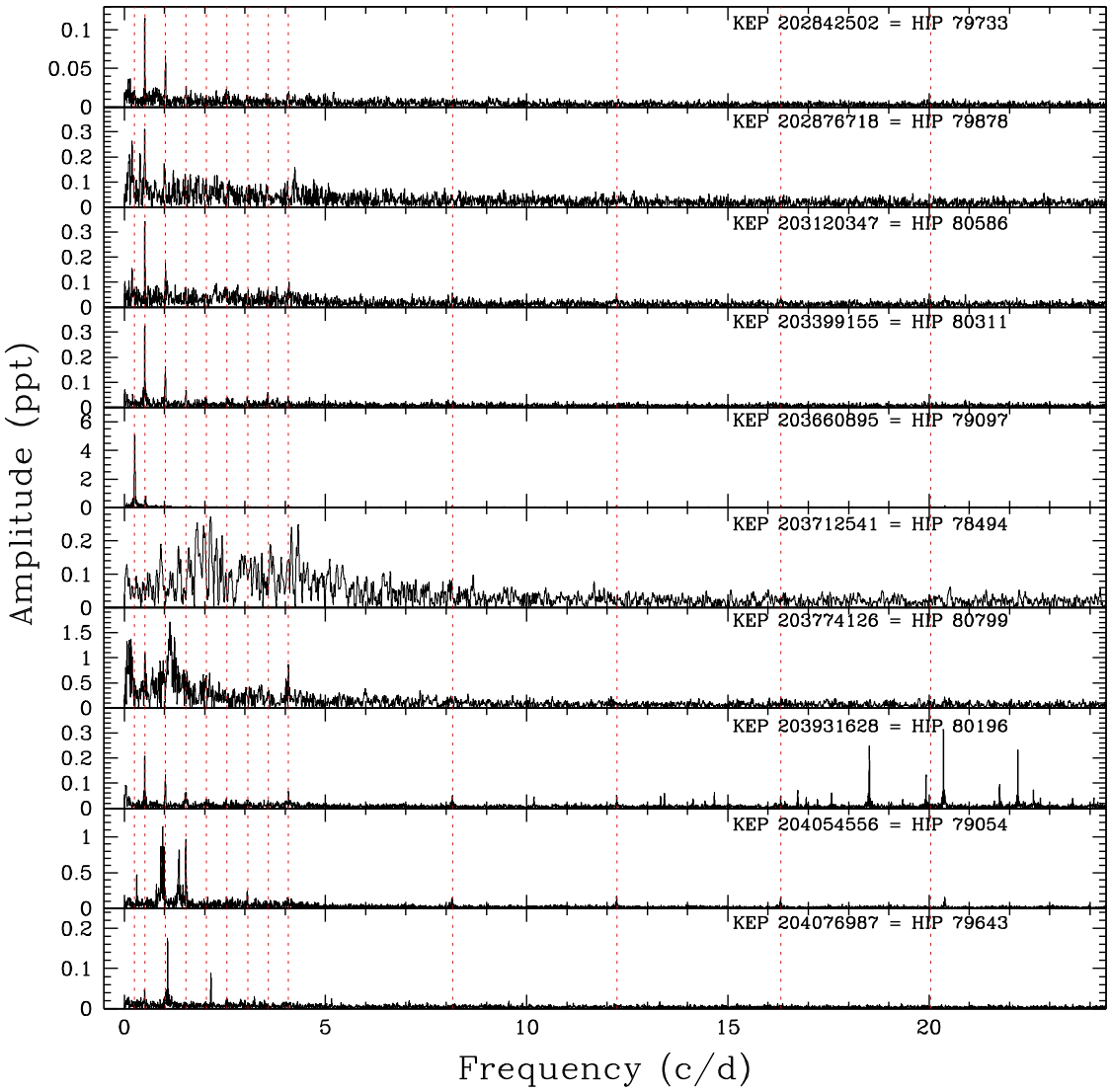

Figure 3. Fourier transform for the 27 objects with LC data. The dashed red lines show frequencies related to the satellite motion.

δ Sct star EPIC 204399980 is one of the least evolved stars of our sample, much younger that the rest. However, the observed position in the HR diagram very close to the zero-age main sequence (ZAMS) runs contrary to this hypothesis, unless the stellar luminosity has been severely underestimated due to a wrong extinction correction.

Considering the other pulsating stars, according to the results of Luhman & Mamajek (2012), EPIC 203931628, 204054556 and 204372172 have a debris/evolved transitional disc, a clear indication of their PMS nature. In the case of EPIC 204175508, 204494885 and 204638251, no infrared excess was found in the literature and thus no evidence for the presence of a circumstellar disc. However, the absence of a significant infrared excess does not necessarily mean that these stars are evolved objects, not belonging to the USco association. Recent studies based both on *Spitzer* photometry up to 70 μm (Carpenter et al. 2006, 2009) and spectroscopy (Dahm & Carpenter 2009) have shown that in general the discs in USco are more evolved than those observed in younger star forming regions. Only ∼20 per cent of the stars have an infrared excess at any wavelength, mostly due to debris rather than primordial discs. On the basis of these considerations, unless the membership evaluation by Pecaut et al. (2012) is wrong, we can consider all the new pulsators as young intermediate-mass stars with an age of ∼10 Myr.

6 THE PULSATING STARS

Recently, Zwintz et al. (2014) have observed a large sample of PMS δ Sct stars and determined their effective temperatures and surface gravities from spectroscopic data. An important result of this study is that the highest observed p-mode frequency, $\nu_{\rm max}$, correlates quite well with the location of the star in the HR diagram since it scales as $gT_{\rm eff}^{-1/2} \sim MT_{\rm eff}^{3.5}L^{-1}$ (see Brown et al. 1991; Kjeldsen & Bedding 1995; Zwintz et al. 2014, for details). The coolest and least-evolved stars (i.e. closest to the birth line) have the lowest values of $\nu_{\rm max}$, while the hottest and most evolved stars (closest to the ZAMS) have the highest values of $\nu_{\rm max}$. Zwintz et al. (2014) interpret the observed trend as due to the behaviour of the acoustic cut-off frequency. The latter is directly proportional to the square root of the star's mean density and therefore it should increase as a star contracts and its density rises. Of course, this property can only be observed in young stars whose radius varies with age. Indeed, for the more evolved, core hydrogen-burning δ Sct stars there is no correlation of $\nu_{\rm max}$ with

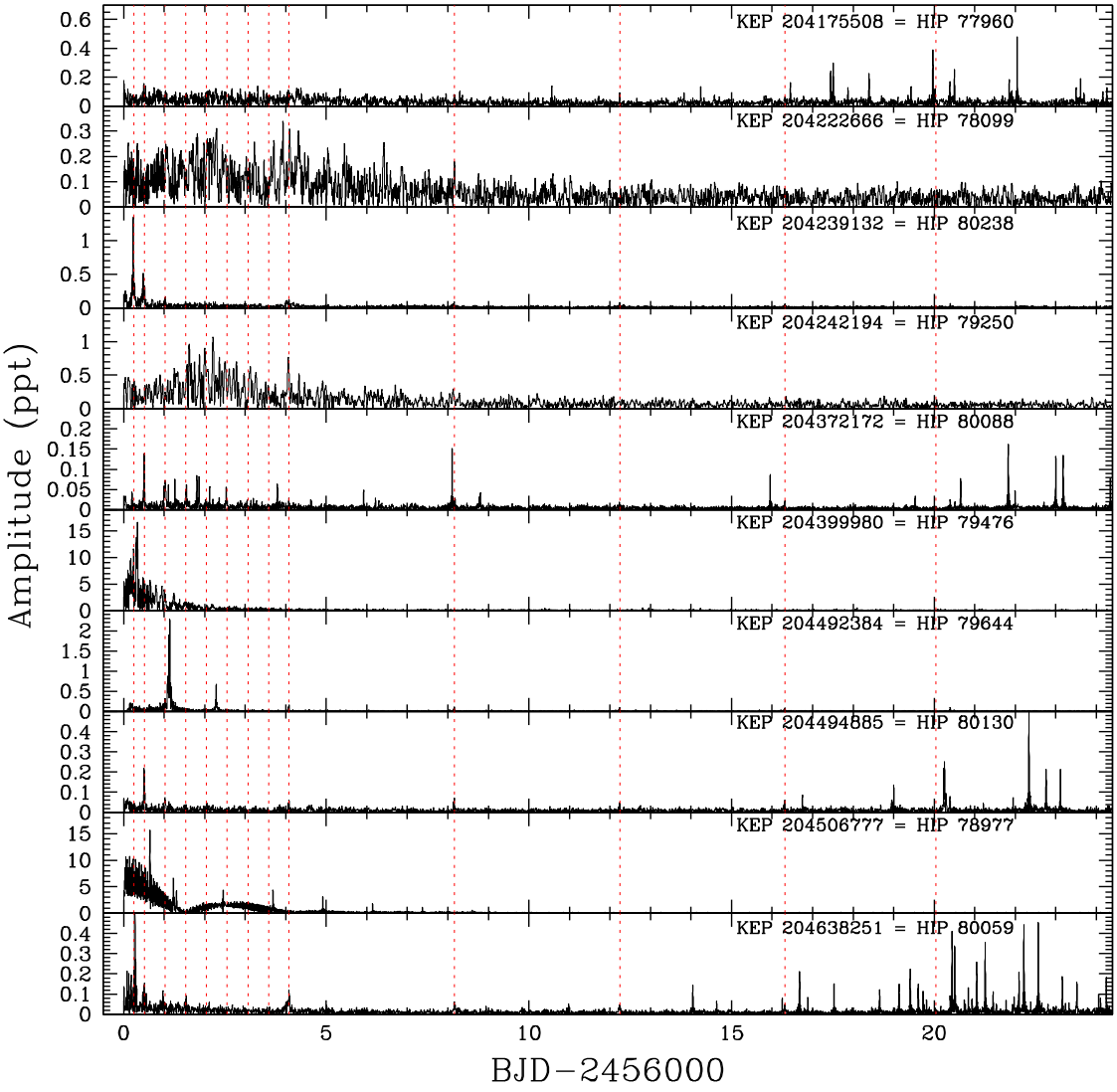

Figure 3 – *continued*

the stellar parameters. Using the observed trend in a homogenous sample of pulsating stars in the young cluster NGC 2264, Zwintz et al. (2014) were able to quantify the age interval during which star formation took place in the parent molecular cloud at the level of at least 5 Myr.

As discussed in Section 3, we have identified six new pulsating stars: namely, EPIC 203931628, 204175508, 204372172, 204399980, 204494885 and 204638251. Unfortunately, since the Nyquist frequency limit of our data is about 24 d^{-1}, the frequencies extracted from the LC mode data are subject to ambiguity preventing an accurate determination of ν_{max}. On the other hand, four stars have been observed in SC mode and in this case we could calculate the values of ν_{max}. It turns out that in all cases $\nu_{max} \sim 42\,d^{-1}$, apart from EPIC 204372172 with $\nu_{max} \approx 33\,d^{-1}$. Furthermore, all these stars have similar properties in terms of effective temperatures and luminosities. Therefore, since the relationship between ν_{max} and the stellar parameters is approximate, we can only draw some qualitative conclusion from the knowledge of the cut-off frequencies.

First, the similar values of ν_{max} could mean that there is little or no age spread in USco among the late A-type stars. Even if EPIC 204372172 has a smaller ν_{max}, the position in the HR diagram is consistent with that of the other stars, preventing us from finding any significant difference in age from the comparison with the isochrones. Secondly, the fact that EPIC 204399980, the star that we consider to be the youngest of our sample on the basis of the presence of a fully developed circumstellar disc, shows a value of ν_{max} as high as that of the other δ Sct stars may appear difficult to interpret. A possibility is that the relation ν_{max}–age found by Zwintz et al. (2014) is not always present in young clusters/associations (Stahler & Palla 2014). Vice versa, and more likely, all the four pulsators of USco have approximately the same age, but EPIC 204399980 somehow managed to maintain its disc for a longer time. This is not an unusual situation considering that actively accreting stars older than 6–8 Myr and still surrounded by circumstellar discs have been found in populous clusters, such as NGC 6611 (De Marchi et al. 2013).

In any case, this result is different from that observed in NGC 2264 studied by (Zwintz et al. 2014). Interestingly, NGC 2264 is known to have a median age of ∼3 Myr, and a significant dispersion of the order of ∼5 Myr (see also Dahm 2008). In the case of USco, the age difference of its members seems to be very small. However, looking at their distribution in the HR

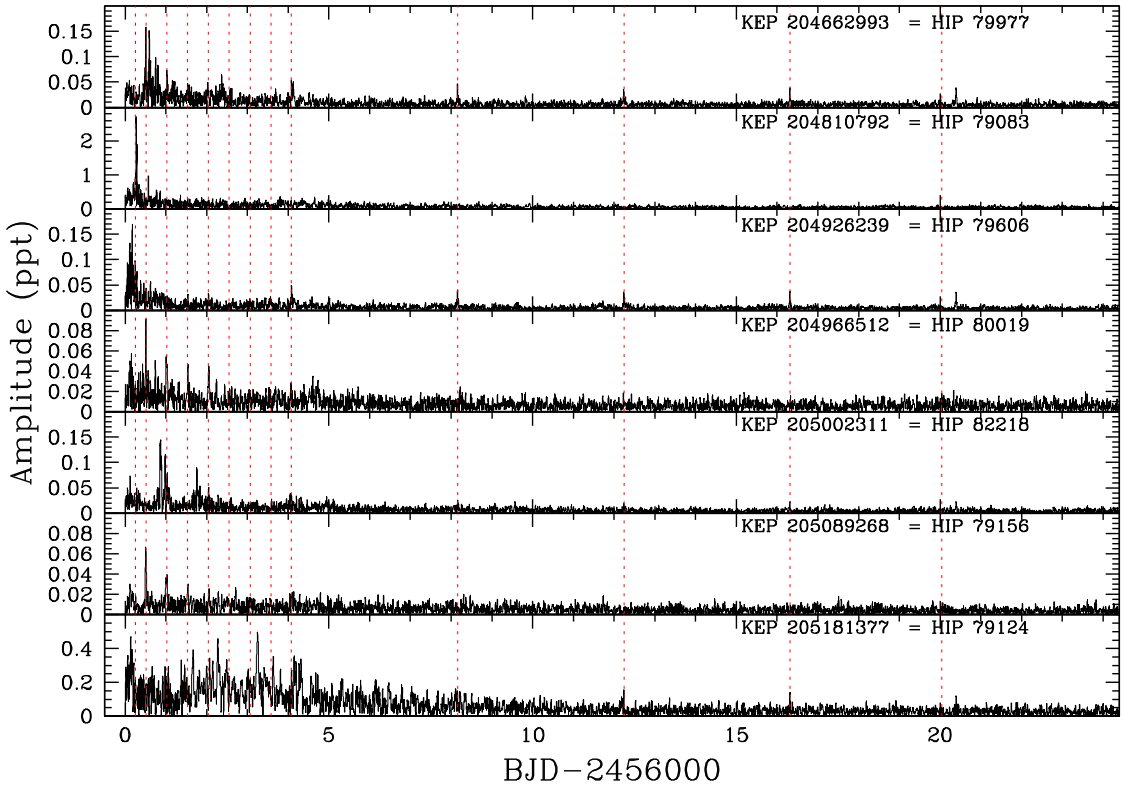

Figure 3 – *continued*

diagram shown in fig. 8, we notice that there are several stars of USco that fall within the instability strip and that lie close to the 5 Myr isochrone (see the light green symbols). Thus, one can argue for an indication of a possible spread in isochronal ages in USco members of the same magnitude of that more solidly derived in NGC 2264. Unfortunately, these putative younger stars have not been observed by *Kepler*, but they are ideal targets for future dedicated observations to search for pulsation and therefore to probe the presence of a possible age spread in this association.

It is interesting to note that low frequencies are almost certainly present in the PMS δ Sct stars discussed here. However, one needs to be careful in making this conclusion because the K2 data are not very reliable at low frequencies due to drift of the stars across the CCD. Nevertheless, the low frequencies in these stars are of sufficiently high amplitude that one can be confident about their identification. The presence of low frequencies is particularly interesting in PMS stars because envelope convection is much more extended in this phase, particularly at early stages when the star radius is still expanded. Therefore, one may expect that the convective blocking mechanism, responsible for the onset of g modes (Guzik et al. 2000), could be more active among these stars. In turn, the study of these low frequency modes is fundamental to investigate the evolutionary status and the internal structure of the intermediate-mass PMS pulsators (Suran et al. 2001).

The independent frequencies extracted for the γ Dor star EPIC 204054556 are listed in Table 3 and displayed in the bottom panel of Fig. 9. In the same figure, we also show for comparison the periodgrams of the two other known PMS γ Dor stars, VAS 20 and VAS 87 in the young cluster NGC 2264 (Zwintz et al. 2013). We see that the frequencies detected in EPIC 20405455 are systematically higher than the γ Dor stars of NGC 2264, a fact that can be attributed to the higher effective temperature of EPIC 20405455. As can be seen in Fig. 8, this star falls well within the instability strip for γ Dor stars, whereas the two variables in NGC 2264 are slightly outside (see Fig. 9 in Zwintz et al. 2013).

As a final consideration, we note that two of the investigated stars, namely EPIC 204239132 and 204242194, do not show any pulsation at a level of $\sim$0.01 ppt, albeit being placed inside the δ Sct instability strip, towards its blue boundary (see Fig. 8). The effective temperature estimate for these stars is not based on solid high-resolution spectroscopy (see Pecaut et al. 2012, and references therein). However, even a 500 K error on the effective temperature cannot place these stars outside the strip. The presence of non-variable stars inside the δ Sct instability strip is a well-known long-standing problem (see e.g. Balona & Dziembowski 2011, and references therein). A recent discussion of this subject is provided by Murphy et al. (2015) whose investigation is based on ultraprecise *Kepler* photometry and high-resolution spectroscopy. Their conclusion is that chemically normal[4] non-variable stars inside the δ Sct instability strip exist but are rare. However, the blue limit of the instability strip used by these authors (i.e. Dupret et al. 2005) is significantly redder than that adopted in this work. As a result, according to Dupret et al. (2005) calculations, EPIC 204239132 and 204242194 would be close or outside the blue boundary of the δ Sct instability strip. In conclusion, given current uncertainties on both effective temperature measurements and instability strip determinations the occurrence of static stars inside the adopted pulsation region cannot be excluded.

[4] In A-type chemically peculiar stars, such as the Am class, a dumping of the pulsation is expected (see e.g. Balona et al. 2011, and references therein).

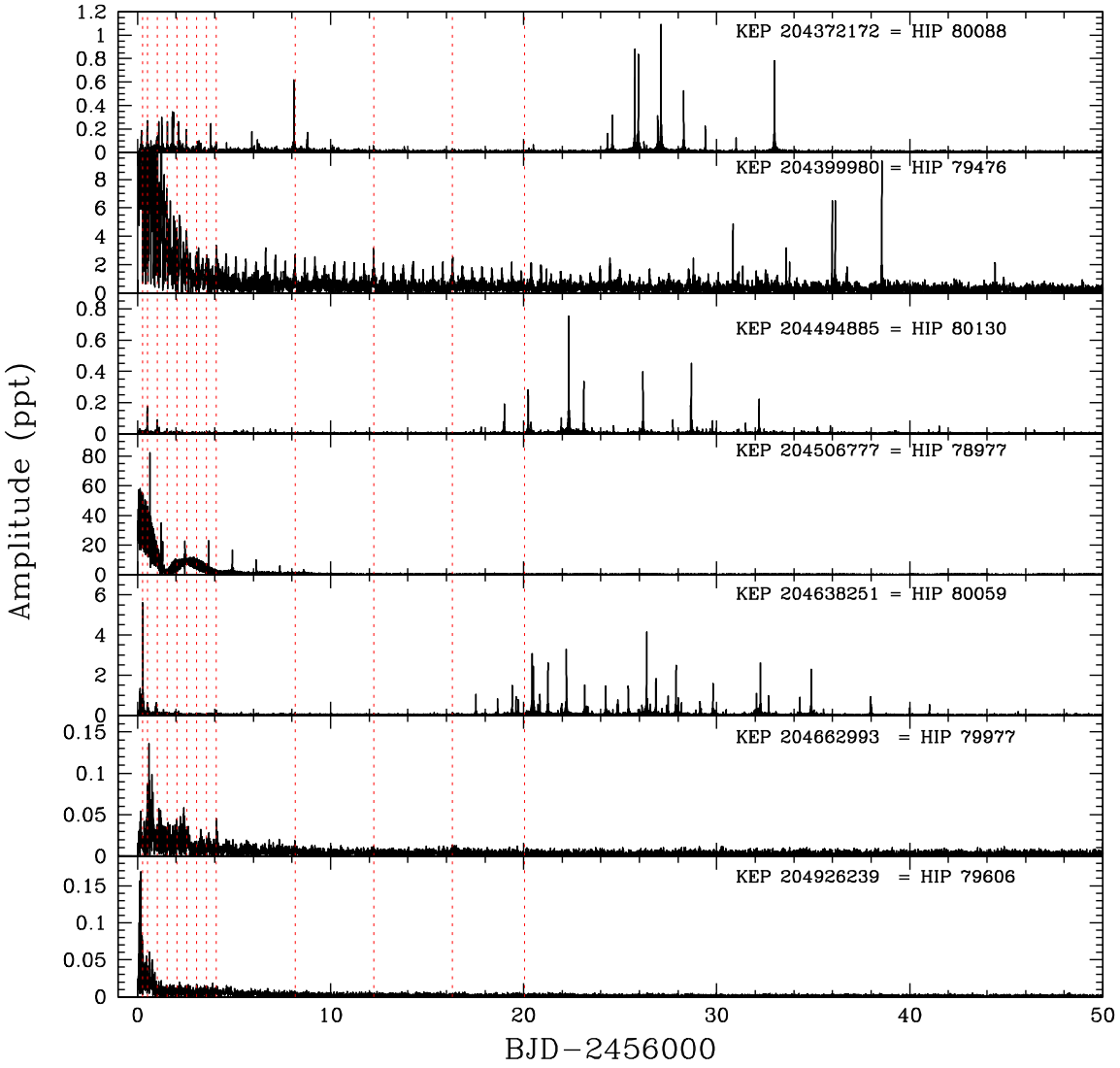

Figure 4. Fourier transform for the seven objects with SC data. The dashed red lines show frequencies related to the satellite motion.

Table 2. Results obtained from the spectroscopic analysis of the sample of stars presented in this work. The different columns show: identification, literature (Pecaut et al. 2012) and spectroscopic effective temperatures, surface gravities ($\log g$), rotational velocities ($v \sin i$), heliocentric julian day of the observations and radial velocities.

EPIC	HIP	$T_{\rm eff}^{\rm Lit}$ (K)	$T_{\rm eff}^{\rm spec}$ (K)	$\log g$	$v \sin i$ (km s^{-1})	JD (245 7100.+)	$V_{\rm rad}$ (km s^{-1})
204506777	78977	6150 ± 150	6300 ± 200	4.10 ± 0.15	80 ± 5	78.4706	15.6 ± 3.0
204399980	79476	7500 ± 200	8100 ± 300	4.00 ± 0.15	110 ± 5	79.4551	−7.4 ± 6.4
204926239	79606	6150 ± 150	6100 ± 150	3.80 ± 0.15	22 ± 2	80.4255	−24.1 ± 1.0
204662993	79977	6700 ± 100	6500 ± 150	4.00 ± 0.15	55 ± 3	85.4380	−6.2 ± 2.7
204638251	80059	7800 ± 250	8000 ± 250	3.95 ± 0.15	90 ± 5	97.3430	7.1 ± 5.7
204372172	80088	7500 ± 150	7600 ± 200	3.80 ± 0.15	80 ± 5	96.4365	−9.1 ± 6.0
204494885	80130	7500 ± 150	8000 ± 250	3.80 ± 0.15	85 ± 5	78.4212	−51.9 ± 6.0

7 CONCLUSIONS

We have presented the light curves obtained with the *Kepler* spacecraft and the derived periodograms of 27 stars belonging to the young Upper Scorpius association. This sample contains only A–F-type stars which are known to be subject to pulsation instability of the δ Sct and γ Dor type during the contraction phase prior to the arrival on the main sequence.

We have identified six new δ Sct variables and one γ Dor star (EPIC 204054556/HIP 79054) which are most likely PMS stars just about to arrive on the ZAMS. Four of the δ Sct variables, namely EPIC 204372172 (HIP 80088) EPIC 204399980

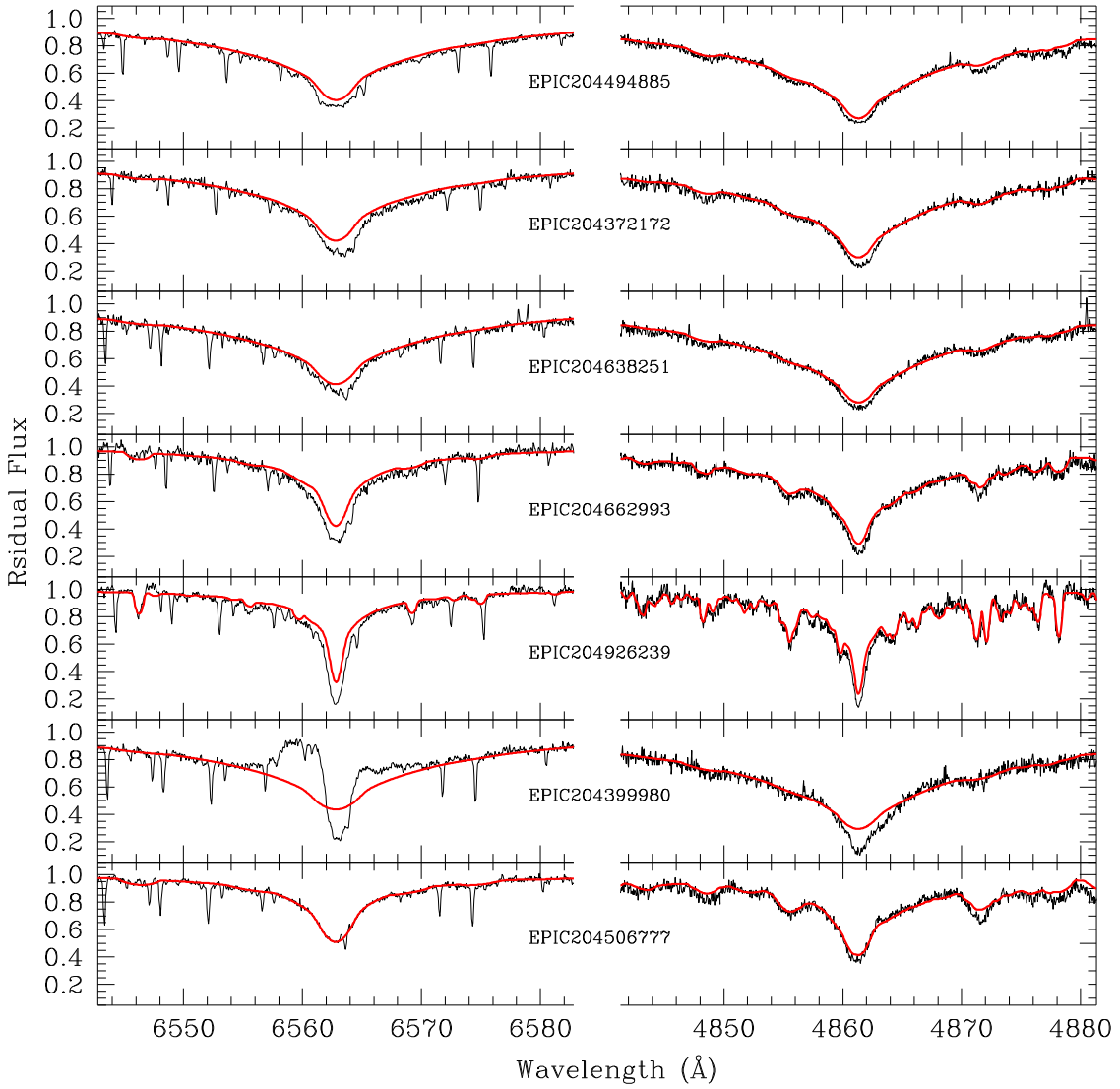

Figure 5. Portions of the spectral echelle orders centred around Hα and Hβ for the program stars. Superposed (red lines) the synthetic spectra computed with the parameters reported in Table 2.

(HIP 79476) EPIC 204494885 (HIP 80130), and EPIC 204638251 (HIP 80059) were also observed in SC mode (time sampling 1-min) allowing us to resolve their entire frequency spectrum. For the remaining two δ Sct stars, EPIC 203931628 (HIP 80196) and EPIC 204175508 (HIP 77960), we only got LC data (time sampling ∼30-min) that were enough to unambiguously identify their variability. Thanks to these new data, USco is the second young cluster after NGC 2264 that hosts several PMS δ Sct/γ Dor variables discovered through space observations.

One of the stars observed in SC, EPIC 204506777 (HIP 78977) appears to be a rotational variable in a hierarchical triple system. This is a particularly important system since future radial velocity measurements will allow us to obtain accurate determination of the mass of the star, thus setting strong constraints on its pulsation properties and on evolutionary models.

Follow-up spectroscopic observations of the newly discovered variables observed in SC allowed us to obtain new estimates of $T_{\rm eff}$, $\log g$, $v \sin i$ and $V_{\rm rad}$. Our second epoch spectroscopy for EPIC 204506777 (the first epoch was obtained from archive data) reveals a significant change of centre-of-mass radial velocity for this star, confirming its multiplicity. However, additional data are required to construct a complete radial velocity curve.

We have used the newly determined stellar parameters of four of the δ Sct stars to place them in the HR diagram and obtain an independent estimate on their age, confirming the value of ∼10 Myr for the members of the USco association. Interestingly, their measured $v \sin i$ values are less or close to ∼100 km s^{-1}, thus the effect of rotation on the pulsation frequencies should be less extreme and the frequency spectra more suitable for comparison with stellar pulsation models (e.g. Ripepi et al. 2011). A quantitative analysis of the new δ Sct and γ Dor stars with the purpose to determine their masses and evolutionary stage will be the subject of a forthcoming paper.

ACKNOWLEDGEMENTS

We thank our anonymous referees for their valuable comments. LAB thanks the SAAO and National Research Foundation of South Africa for financial support. This work made use of PYKE (Still & Barclay 2012), a software package for the reduction and

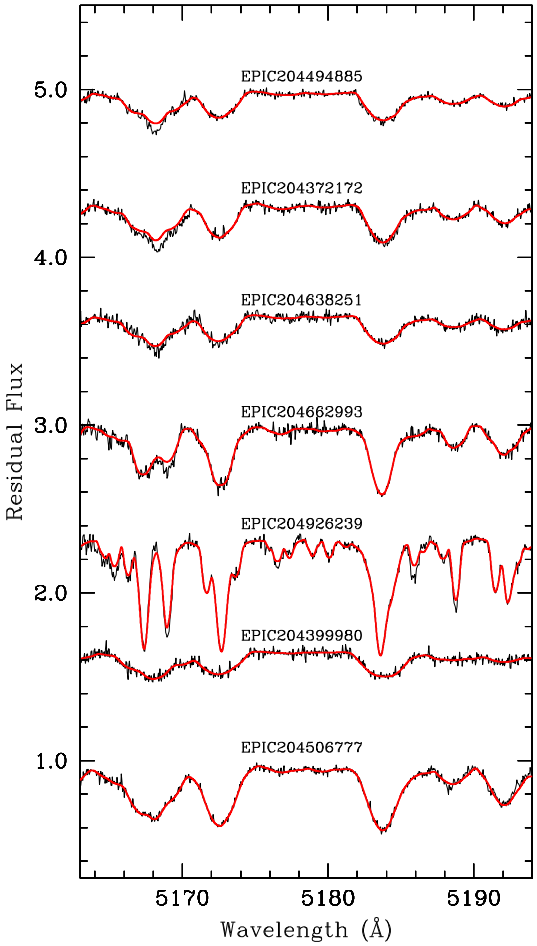

Figure 6. Spectral synthesis in the range of the Mg I triplet 5150–5200 Å.

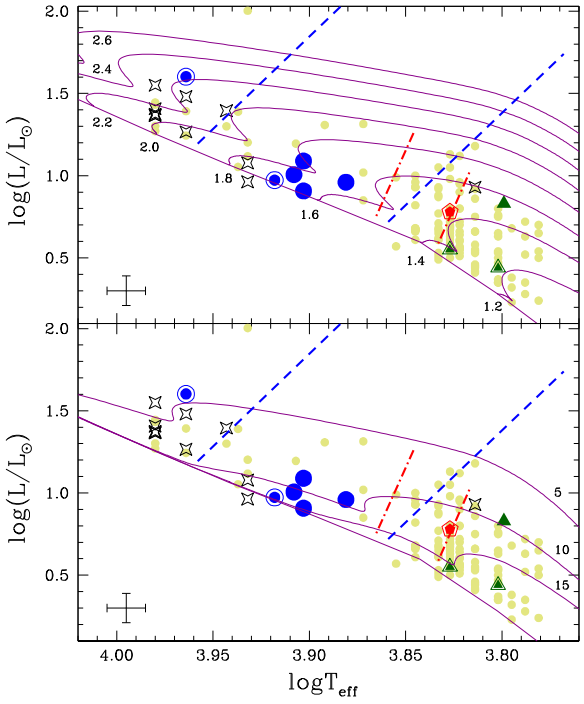

Figure 8. HR diagram for the A–F stars members of the USco association according to Pecaut et al. (2012) except for the four δ Sct observed with CAOS. For these stars, we used the results of Table 2. Light green symbols show objects not observed by *Kepler*. Black four-starred symbols represent constant stars. Green triangles, red pentagons and blue circles show binary/rotational, γ Dor variables and δ Sct, respectively. For these variables, empty-filled and filled symbols represent data possessing only LC and LC–SC cadences, respectively. For comparison purposes, we overplot the δ Sct (blue dashed lines) and the theoretical edges of the γ Dor (red dot–dashed lines) instability strips by Breger & Pamyatnykh (1998) and Warner, Kaye & Guzik (2003), respectively. We note that the mixing-length parameter adopted in the computation of γ Dor instability strip was 1.87. The solid lines in the top panel show the ZAMS and selected evolutionary tracks from Tognelli et al. (2011). Similarly, in the bottom panel solid lines show isochrones for 5,10 and 15 Myr as taken from the same authors. The evolutionary models and isochrones were calculated for a solar mixture with $Z = 0.015$, $Y = 0.278$ and mixing length = 1.68.

analysis of *Kepler* data. This open-source software project is developed and distributed by the NASA Kepler Guest Observer Office. This research has made use of the SIMBAD data base and VizieR catalogue access tool, operated at CDS, Strasbourg, France. We gratefully acknowledge the *Kepler* team and the Guest Observer Office whose outstanding efforts have made these results possible.

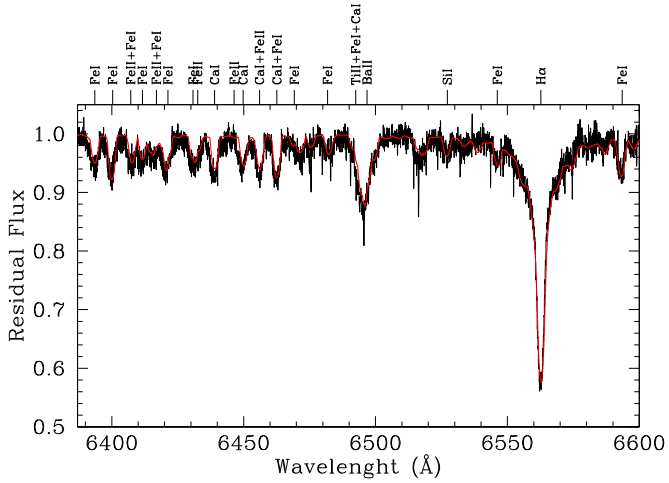

Figure 7. Portion of the spectral echelle order in the region of Hα for HIP 78977. Superposed (red line) the synthetic spectra computed with the parameters reported in Table 2.

Table 3. List of pulsation frequencies and amplitudes for the four candidate PMS δ Sct stars observed in SC mode. EPIC 204054556 is a candidate γ Dor star. Given the problematic light curve at low frequencies, for star EPIC 204399980, only frequencies larger than 10 d^{-1} are listed. Errors on each value of frequency and amplitude are shown within parenthesis.

n	ν_n d^{-1}	A_n ppt	n	ν_n d^{-1}	A_n ppt
	EPIC 204638251			**EPIC 204494885**	
1	26.3734(1)	4.09(1)	1	22.3371(1)	0.741(2)
2	22.2123(1)	3.20(1)	2	28.6862(1)	0.445(2)
3	20.4388(1)	2.99(1)	3	26.1806(1)	0.395(2)
4	21.2569(1)	2.57(1)	4	23.1134(1)	0.332(2)
5	32.2632(1)	2.57(1)	5	20.2332(1)	0.277(2)
6	27.8936(1)	2.46(1)	6	32.1927(1)	0.216(2)
7	34.8966(1)	2.28(1)	7	19.0010(1)	0.191(2)
8	20.5055(1)	2.28(1)	9	28.6459(1)	0.150(2)
9	26.8491(1)	1.83(1)	10	21.9472(2)	0.102(2)
10	29.8055(1)	1.59(1)	11	27.7289(2)	0.088(2)
11	23.1606(1)	1.50(1)	12	18.9506(2)	0.081(2)
12	19.4065(1)	1.45(1)	13	29.7855(2)	0.079(2)
13	25.4210(1)	1.43(1)	14	20.3818(2)	0.079(2)
14	2 4.2454(1)	1.38(1)	15	31.4909(2)	0.070(2)
15	32.0598(1)	1.11(1)	16	35.8862(3)	0.055(2)
16	20.8422(1)	1.06(1)	17	24.6552(3)	0.050(2)
17	17.5276(1)	1.04(1)	18	41.5304(3)	0.046(2)
18	27.4845(1)	1.00(1)	19	17.8007(3)	0.045(2)
19	32.6900(1)	0.99(1)	20	28.9853(4)	0.044(2)
20	28.0091(1)	0.89(1)	21	35.2287(4)	0.041(2)
21	34.3108(1)	0.89(1)	22	23.5385(4)	0.037(2)
22	19.6051(1)	0.88(1)	23	25.4051(4)	0.036(2)
23	37.9624(1)	0.87(1)	24	29.9793(5)	0.034(2)
24	18.6522(1)	0.81(1)	25	40.9774(5)	0.029(2)
25	19.7238(1)	0.77(1)	26	31.1484(5)	0.029(2)
26	24.8841(1)	0.73(1)	27	29.4519(5)	0.029(2)
27	29.1318(1)	0.68(1)	28	31.0579(6)	0.027(2)
28	28.1713(2)	0.58(1)	29	29.6588(6)	0.027(2)
29	21.9698(2)	0.58(1)			
30	41.0177(2)	0.56(1)		**EPIC 204054556**	
31	24.8410(2)	0.54(1)	1	0.9547(4)	0.94(3)
32	27.4063(2)	0.52(1)	2	1.3645(4)	0.84(3)
33	38.0033(2)	0.52(1)	3	0.9129(4)	0.91(3)
34	23.2401(2)	0.48(1)	4	0.9907(4)	0.82(3)
35	26.1315(2)	0.47(1)	5	1.3433(4)	0.73(3)
36	26.5991(2)	0.45(1)	6	0.9743(5)	0.46(3)
37	20.7439(2)	0.45(1)	7	0.3096(5)	0.50(3)
38	22.2047(2)	0.39(1)	8	0.9346(5)	0.53(3)
	EPIC 204372172			**EPIC 204399980**	
1	27.1136(1)	1.073(5)	1	38.5484(1)	9.11(2)
2	25.7598(1)	0.869(5)	2	36.1364(1)	6.39(2)
3	25.9414(1)	0.819(5)	3	35.9815(1)	6.09(2)
4	32.9888(1)	0.770(5)	4	33.7720(2)	2.51(2)
5	28.2886(1)	0.520(5)	5	28.7870(2)	2.28(2)
6	24.5972(1)	0.315(5)	6	44.4148(2)	1.98(2)
7	26.9462(1)	0.311(5)	7	31.1505(2)	1.82(2)
8	29.4115(2)	0.227(5)	9	36.7527(2)	1.72(2)
9	24.3411(2)	0.156(5)	10	21.1801(2)	1.69(2)
10	31.0072(3)	0.119(5)	11	32.5195(2)	1.26(2)
11	26.2301(4)	0.098(5)	12	28.8649(3)	1.06(2)
12	20.5083(5)	0.066(5)	13	28.8440(3)	0.79(2)
			14	27.5603(3)	0.68(2)
			15	25.6695(4)	0.55(2)
			16	23.4758(4)	0.46(2)
			17	17.3511(5)	0.38(2)
			18	38.7263(5)	0.38(2)
			19	36.1503(5)	0.38(2)

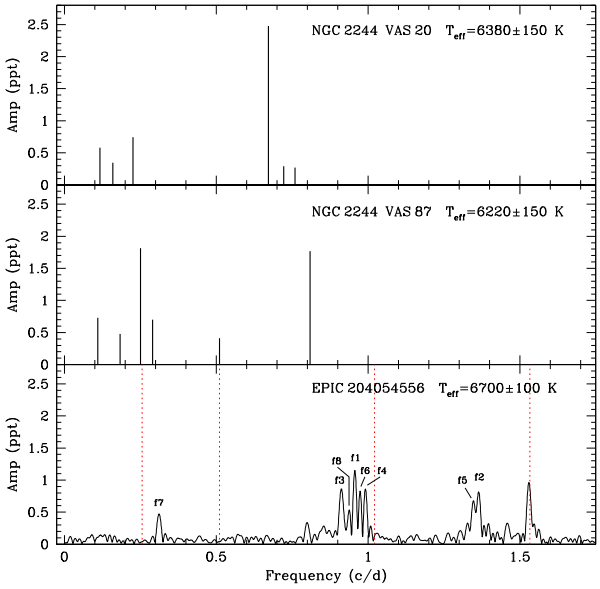

Figure 9. Top and medium panels show the schematic periodograms of the PMS γ Dor variables VAS 20 and VAS 87 in NGC 2244 (Zwintz et al. 2013). Bottom panel displays the periodogram of the candidate γ Dor variable in USco, EPIC 204054556. The labels corresponds to the frequencies listed in Table 3. The dashed lines show the instrumental frequencies.

This paper includes data collected by the *Kepler* mission. Funding for the *Kepler* mission is provided by the NASA Science Mission directorate. All of the data presented in this paper were obtained from the Mikulski Archive for Space Telescopes (MAST). STScI is operated by the Association of Universities for Research in Astronomy, Inc, under NASA contract NAS5-26555. Support for MAST for non-*HST* data is provided by the NASA Office of Space Science via grant NNX09AF08G and by other grants and contracts.

REFERENCES

Balona L. A., 2014, MNRAS, 437, 1476
Balona L. A., Dziembowski W. A., 2011, MNRAS, 417, 591
Balona L. A. et al., 2011, MNRAS, 414, 792
Baraffe I., Chabrier G., Allard F., Hauschildt P. H., 2002, A&A, 382, 563
Breger M., Pamyatnykh A. A., 1998, A&A, 332, 958
Brown T. M., Gilliland R. L., Noyes R. W., Ramsey L. W., 1991, ApJ, 368, 599
Carmona A., van den Ancker M. E., Audard M., Henning T., Setiawan J., Rodmann J., 2010, A&A, 517, A67
Carpenter J. M., Mamajek E. E., Hillenbrand L. A., Meyer M. R., 2006, ApJ, 651, L49
Carpenter J. M., Mamajek E. E., Hillenbrand L. A., Meyer M. R., 2009, ApJ, 705, 1646
Casey M. P. et al., 2013, MNRAS, 428, 2596
Catanzaro G., Balona L. A., 2012, MNRAS, 421, 1222
Catanzaro G., Ripepi V., 2014, MNRAS, 441, 1669
Catanzaro G. et al., 2011, MNRAS, 411, 1167
Catanzaro G., Ripepi V., Bruntt H., 2013, MNRAS, 431, 3258
Catanzaro G. et al., 2015, MNRAS, 451, 4703
Dahm S. E., 2008, in Reipurth B., ed., ASP Monograph Publications, Vol. 1, Handbook of Star Forming Regions, Volume I: The Northern Sky. ASP Monograph Publ., San Francisco, CA, p. 966
Dahm S. E., Carpenter J. M., 2009, AJ, 137, 4024
de Bruijne J. H. J., 1999, MNRAS, 310, 585
De Marchi G., Panagia N., Guarcello M. G., Bonito R., 2013, MNRAS, 435, 3058

de Zeeuw P. T., Hoogerwerf R., de Bruijne J. H. J., Brown A. G. A., Blaauw A., 1999, AJ, 117, 354
Di Criscienzo M., Ventura P., D'Antona F., Marconi M., Ruoppo A., Ripepi V., 2008, MNRAS, 389, 325
Dotter A., Chaboyer B., Jevremović, Kostov V., Baron E., Ferguson J. W., 2008, ApJS, 178, 89
Doyle A. P., Davies G. R., Smalley B., Chaplin W. J., Elsworth Y., 2014, MNRAS, 444, 3592
Dupret M.-A., Grigahcène A., Garrido R., Gabriel M., Scuflaire R., 2005, A&A, 435, 927
Guzik J. A., Kaye A. B., Bradley P. A., Cox A. N., Neuforge C., 2000, ApJ, 542, L57
Herbst W., Herbst D. K., Grossman E. J., Weinstein D., 1994, AJ, 108, 1906
Hillenbrand L. A., White R. J., 2004, ApJ, 604, 741
Houk N., Smith-Moore M., 1988, Michigan Catalogue of Two-Dimensional Spectral Types for the HD Stars. 4. Declinations −26°.0 to −12°.0. Department of Astronomy, University of Michigan
Hubrig S. et al., 2014, MNRAS, 442, 3604
Kiraga M., 2012, Acta Astron., 62, 67
Kjeldsen H., Bedding T. R., 1995, A&A, 293, 87
Kurucz R. L., 1993a, in Dworetsky M. M., Castelli F., Faraggiana R., eds, ASP Conf. Ser. Vol. 44, IAU Colloq. 138:A New Opacity-Sampling Model Atmosphere Program for Arbitrary Abundances. Astron. Soc. Pac., San Francisco, p. 87
Kurucz R. L., 1993b, ATLAS9 Stellar Atmosphere Programs and 2 km/s grid, Kurucz CD-ROM 13: ATLAS9, Smithsonian Astrophysical Observatory, Cambridge, MA
Kurucz R. L., 1997, in Philip A. G. D., Liebert J., Saffer R., Hayes D. S., eds, The Third Conference on Faint Blue Stars, Davis Press, Schenectady, NY, p. 33
Kurucz R. L., Avrett E. H., 1981, SAO Special Rep. 391
Lenz P., Breger M., 2005, Commun. Astroseismol., 146, 53
Luhman K. L., Mamajek E. E., 2012, ApJ, 758, 31
Marconi M., Palla F., 1998, ApJ, 507, L141
Marconi M., Palla F., 2004, in Zverko J., Weiss W. W., Ziznovsky J., Adelman S. J., eds, Proc. IAU Symp. 224, The A-Star Puzzle. Cambridge Univ. Press, Cambridge, p. 69
Murphy S. J., Bedding T. R., Niemczura E., Kurtz D. W., Smalley B., 2015, MNRAS, 447, 3948
Niemczura E. et al., 2015, MNRAS, 450, 2764
Palla F., Stahler S. W., 1999, ApJ, 525, 772
Paunzen E., Skarka M., Holdsworth D. L., Smalley B., West R. G., 2014, MNRAS, 440, 1020
Pecaut M. J., Mamajek E. E., Bubar E. J., 2012, ApJ, 746, 154
Ripepi V., Palla F., Marconi M., Bernabei S., Arellano Ferro A., Terranegra L., Alcalá J. M., 2002, A&A, 391, 587
Ripepi V. et al., 2003, A&A, 408, 1047
Ripepi V., Marconi M., Palla F., Bernabei S., Ruoppo A., Cusano F., Alcalá J. M., 2006a, Mem. Soc. Astron. Ital., 77, 317
Ripepi V. et al., 2006b, A&A, 449, 335
Ripepi V. et al., 2011, MNRAS, 416, 1535
Ruoppo A., Marconi M., Marques J. P., Monteiro M. J. P. F. G., Christensen-Dalsgaard J., Palla F., Ripepi V., 2007, A&A, 466, 261
Sbordone L., Bonifacio P., Castelli F., Kurucz R. L., 2004, Mem. Soc. Astron. Ital. Suppl., 5, 93
Siess L., Dufour E., Forestini M., 2000, A&A, 358, 593
Stahler S., Palla F., 2014, Science, 345, 514
Still M., Barclay T., 2012, Astrophysics Source Code Library, record ascl:1208.004
Suran M., Goupil M., Baglin A., Lebreton Y., Catala C., 2001, A&A, 372, 233
Tognelli E., Prada Moroni P. G., Degl'Innocenti S., 2011, A&A, 533, A109
Valenti J. A., Piskunov N., 1996, A&AS, 118, 595
van den Ancker M. E., de Winter D., Tjin A Djie H. R. E., 1998, A&A, 330, 145
Vanderburg A., Johnson J. A., 2014, PASP, 126, 948
Vieira S. L. A., Corradi W. J. B., Alencar S. H. P., Mendes L. T. S., Torres C. A. O., Quast G. R., Guimarães M. M., da Silva L., 2003, AJ, 126, 297
Warner P. B., Kaye A. B., Guzik J. A., 2003, ApJ, 593, 1049
Zwintz K., 2008, ApJ, 673, 1088
Zwintz K., Fossati L., Ryabchikova T., Kaiser A., Gruberbauer M., Barnes T. G., Baglin A., Chaintreuil S., 2013, A&A, 550, A121
Zwintz K. et al., 2014, Science, 345, 550

This paper has been typeset from a TEX/LATEX file prepared by the author.